Smart Structures and Systems, *Vol. 17, No. 2 (2016) 257-274*
DOI: http://dx.doi.org/10.12989/sss.2016.17.2.257

On bending, buckling and vibration of graphene nanosheets based on the nonlocal theory

Jinjian Liu, Ling Chen, Feng Xie, Xueliang Fan and Cheng Li*

School of Urban Rail Transportation, Soochow University, Suzhou 215131, China

(Received July 6, 2015, Revised November 25, 2015, Accepted December 8, 2015)

Abstract. The nonlocal static bending, buckling, free and forced vibrations of graphene nanosheets are examined based on the Kirchhoff plate theory and Taylor expansion approach. The nonlocal nanoplate model incorporates the length scale parameter which can capture the small scale effect. The governing equations are derived using Hamilton's principle and the Navier-type solution is developed for simply-supported graphene nanosheets. The analytical results are proposed for deflection, natural frequency, amplitude of forced vibration and buckling load. Moreover, the effects of nonlocal parameter, half wave number and three-dimensional sizes on the static, dynamic and stability responses of the graphene nanosheets are discussed. Some illustrative examples are also addressed to verify the present model, methodology and solution. The results show that the new nanoplate model produces larger deflection, smaller circular frequencies, amplitude and buckling load compared with the classical model.

Keywords: bending; buckling; free vibration; forced vibration; nonlocal theory; graphene nanosheets

1. Introduction

With the rapid development of current nano-electro-mechanical systems, the mechanical properties of some common nano-structures including carbon nanotube and graphene nanosheet are required to be well characterized to control their assemblage and optimization. When material scale down to nanometer level, the small scale, surface and quantum effects become significant which should be taken into consideration (Eberhardt and Wallmersperger 2014). The classical continuum mechanics theory has been proved to be not capable of describing the nano-structures because the classical theory lacks the length scale parameter which reveals the small scale effect. Atomic theory is one choice to replace classical theory to study the mechanical properties of nano-structures. However, some nano-systems are too large to describe via the atomic theory. For example, molecular dynamics and Monte Carlo simulations are currently only able to calculate the system containing tens of thousands of atoms. On the other hand, some new continuum theories considering small scale effect are developed to predict nano-structural mechanical behaviors, where the nonlocal theory initiated by Eringen has been widely utilized in nano-mechanics. In such nonlocal theory, the small-scale effect is captured by assuming the stress at a point as a function not only of the strain at that point but also a function of the strains at all other points in

*Corresponding author, Ph. D., Associate Professor, E-mail: licheng@suda.edu.cn

http://www.techno-press.org/?journal=sss&subpage=8 ISSN: 1738-1584 (Print), 1738-1991 (Online)

the domain (Eringen and Edelen 1972, Eringen, 1983). Consequently, the nonlocal theory contains information about the long-range forces between atoms and the internal length scale is introduced into the higher-order constitutive equation. By introducing higher-order derivatives and Green's function into the original integral constitutive relation, an equivalent differential constitutive equation was deduced by Eringen. Since then, the differential nonlocal theory has been applied in nano-mechanics extensively with increasing publications during past decades.

At present, one-dimensional nanostructured materials such as carbon nanotubes and nanobeams have been sufficiently investigated in the promotion of nanotechnology. For example, Reddy (2007) used different beam theories including those of Euler-Bernoulli, Timoshenko, Levinson and Reddy to analyze bending, buckling and vibration of nonlocal beams. Aydogdu (2009) proposed a generalized nonlocal beam theory to study bending, buckling, and free vibration of nanobeams. Murmu and Pradhan (2009) investigated vibration response of nanocantilever considering nonuniformity in the cross sections based on nonlocal elasticity theory. Li *et al.* (2011) studied the transverse dynamical responses and stabilities of nanobeams subjected to a variable axial load based on nonlocal elasticity theory. Şimşek and Yurtcu (2013) examined static bending and buckling of a functionally graded nanobeam based on the nonlocal Timoshenko and Euler–Bernoulli beam theory. The size-dependent static-buckling behaviors of functionally graded nanobeams were investigated by Eltaher *et al.* (2013) on the basis of the nonlocal continuum model. The vibration and stability analysis of a single-walled carbon nanotube conveying nanoflow embedded in biological soft tissue were performed by Hosseini *et al.* (2014). Yin *et al.* (2015) applied the Euler-Bernoulli beam theory, surface elastic theory, the strain equivalent assumption and modified couple stress theory to derive the nonlinear governing equations of the nano-beam. In their work (Yin *et al.* 2015), the Galerkin method and the harmonic balance method were adopted so as to give a solution to the equations.

Due to their extraordinary mechanical, physical and chemical properties, such as low weight, high surface area and extremely high stiffness, two-dimensional nanostructured materials such as graphene nanosheets have attracted increased interest in recent years. After carbon nanotubes, it is expected for graphene nanosheets to trigger a revolution in the modern electronic technology field. Therefore, research and analyses on the mechanical properties and stabilities of graphene nanosheets are indispensable. Liew *et al.* (2006) proposed a continuum-based plate model to study the vibration behaviors of multi-layered graphene nanosheets which are embedded in an elastic matrix. The vibration of orthotropic single layered graphene nanoplates was analyzed using nonlocal elasticity theory and the small scale effect was discussed by Pradhan and Phadikar (2009) and Pradhan and Kumar (2011). The potential of single-layered graphene nanosheet as a nanomechanical sensor was explored by Shen *et al.* (2012). Dynamic pull-in instability and free vibration characteristics of circular higher-order shear deformable nanoplates subjected to hydrostatic and electrostatic forces including surface stress effect were studied by Sahmani and Bahrami (2015). Yan *et al.* (2015) applied the nonlocal continuum mechanics to derive a complete and asymptotic representation of the infinite higher-order governing differential equations for nanobeam and nanoplate models. Bedroud *et al.* (2015) provided the axisymmetric/asymmetric buckling analysis of moderately thick circular and annular functionally graded nanoplates under uniform compressive in-plane loads. Hosseini-Hashemi *et al.* (2015) presented analytical closed-form solutions in explicit forms to investigate small scale effects on the buckling and the transverse vibration behaviors of Levy-type rectangular nanoplates based on the Reddy's nonlocal third-order shear deformation plate theory. Based on an element-free kp-Ritz method, Zhang et al. (2015) developed a nonlocal continuum model for vibration of single-layered graphene nanosheets.

Further, Zhang *et al*. (2015) performed the transient analyses of single-layered graphene nanosheet using the element-free kp-Ritz method and nonlocal elasticity theory.

In the present study, nonlocal Kirchhoff nanoplate model is employed to analyze bending, buckling and vibration of graphene nanosheets using of Taylor expansion approach. In particular, the forced vibration of graphene nanosheets is investigated in detail. Governing equations are derived based on the Hamilton's principle. Numerical results for simply supported graphene nanosheets are presented to examine the validity and accuracy of the method suggested in this paper. Further more, the effects of nonlocal parameter, half wave number and three-dimensional sizes on different responses of graphene nanosheets are demonstrated.

2. Nonlocal nanoplate model for graphene nanosheets

According to the nonlocal elasticity theory, the stress components at a position x depend not only on the strain components at the same position x but also on all other points of the body. Hence, the basic constitutive equations for an isotropic, homogeneous linear nonlocal elastic solid without body force are given by Eringen (1983)

$$\sigma_{ij,j} = 0 \tag{1a}$$

$$\sigma_{ij}(x) = \int \lambda\left(|x - x'|, \alpha\right) C_{ijkl}\varepsilon_{kl}\left(x'\right) dV\left(x'\right), \forall x \in \vee \tag{1b}$$

$$\varepsilon_{ij} = \frac{1}{2}(u_{i,j} + u_{j,i}) \tag{1c}$$

where σ_{ij} and ε_{ij} are nonlocal stress and strain tensors respectively, C_{ijkl} is the fourth-order elasticity tensor, u_i is the displacement vector, $\lambda\left(|x - x'|, \alpha\right)$ is the nonlocal modulus or attenuation function incorporating into constitutive equations the nonlocal effects at the reference point x produced by local strain at the source x'; $|x'-x|$ represents the distance in Euclidean form and α is a material constant that depends on internal (e.g., lattice parameter, granular size, distance between C–C bonds) and external characteristics lengths (e.g., crack length, wave length).

Since the integral constitutive Eq. (1b) is difficult to solve, a simplified equation in differential form was proposed as a basis of all nonlocal constitutive formulation (Eringen 1983)

$$\left[1 - \left(e_0 a\right)^2 \nabla^2\right] \sigma_{ij} = \sigma'_{ij} \tag{2}$$

where $\nabla^2 = \frac{\partial^2}{\partial x^2} + \frac{\partial^2}{\partial y^2}$ is Laplacian operator and σ'_{ij} denotes the local or classical stress, e_0 is a constant for adjusting the model in matching some reliable results by experiments or other models, a is the internal length scale.

Using Taylor expansion, Eq. (2) can be rewritten as

$$\sigma'_{ij} = \frac{1}{\left[1-\left(e_0 a\right)^2 \nabla^2\right]\frac{1}{\sigma_{ij}}} = \sigma_{ij} + \left(e_0 a\right)^2 \nabla^2 \sigma_{ij} + \left(e_0 a\right)^4 \nabla^4 \sigma_{ij} + \mathrm{L} = \sum_{k=0}^{\infty} \left(e_0 a\right)^{2k} \nabla^{2k} \sigma_{ij} \tag{3}$$

Force and moment resultants of nonlocal elasticity can be defined as

$$\left\{N_{xx},\, N_{xy},\, N_{yy}\right\} = \int_{-\frac{h}{2}}^{\frac{h}{2}} \left(\sigma_{xx},\, \sigma_{xy},\, \sigma_{yy}\right) dz \tag{4}$$

$$\left\{M_{xx},\, M_{xy},\, M_{yy}\right\} = \int_{-\frac{h}{2}}^{\frac{h}{2}} \left(\sigma_{xx},\, \sigma_{xy},\, \sigma_{yy}\right) z dz \tag{5}$$

Upon denoting displacement components u_1, u_2 and u_3 along the *x*, *y* and *z* directions, respectively, the displacement field is derived according to the classical Kirchhoff plate theory as

$$u_1\left(x,\, y,\, z,\, t\right) = u\left(x,\, y,\, t\right) - z\,\frac{\partial w}{\partial x} \tag{6a}$$

$$u_2\left(x,\, y,\, z,\, t\right) = v\left(x,\, y,\, t\right) - z\,\frac{\partial w}{\partial y} \tag{6b}$$

$$u_3\left(x,\, y,\, z,\, t\right) = w\left(x,\, y,\, t\right) \tag{6c}$$

where *u*, *v* and *w* are the displacement functions of the middle surface of the nanoplate, and *t* denotes time.

The stain filed can be expressed as

$$\varepsilon_{xx} = \frac{\partial u}{\partial x} - z\,\frac{\partial^2 w}{\partial x^2} \tag{7a}$$

$$\varepsilon_{yy} = \frac{\partial v}{\partial y} - z\,\frac{\partial^2 w}{\partial y^2} \tag{7b}$$

$$\varepsilon_{xy} = \frac{\partial u}{\partial y} + \frac{\partial v}{\partial x} - 2z\,\frac{\partial^2 w}{\partial x \partial y} \tag{7c}$$

Using Eq. (3), the stress constitutive relation of graphene nanoplate model can be written as

$$\begin{Bmatrix} \sigma_{xx} \\ \sigma_{xy} \\ \sigma_{yy} \end{Bmatrix} = \begin{bmatrix} \frac{E}{1-\mu^2} & 0 & \frac{\mu E}{1-\mu^2} \\ 0 & \mathrm{G} & 0 \\ \frac{\mu E}{1-\mu^2} & 0 & \frac{E}{1-\mu^2} \end{bmatrix} \begin{Bmatrix} \sum_{k=0}^{\infty} \left(e_0 a\right)^{2k} \nabla^{2k} \varepsilon_{xx} \\ \sum_{k=0}^{\infty} \left(e_0 a\right)^{2k} \nabla^{2k} \varepsilon_{xy} \\ \sum_{k=0}^{\infty} \left(e_0 a\right)^{2k} \nabla^{2k} \varepsilon_{yy} \end{Bmatrix} \tag{8}$$

where *E*, *G* and μ denote elastic modulus, shear modulus and Poisson's ration, respectively.

Consider a rectangular nanoplate with the length *a*, width *b* and thickness *h*. The Cartesian coordinate system (*x*,*y*,*z*) is constructed to derive mathematical formulations while *x* and *y* coordinates are located in the bottom plane of plate. The governing equations of the graphene nanosheets are extracted based on Hamilton's principle, given as

$$\int_0^T \left(\delta K - (\delta U - \delta W)\right) dt = 0 \tag{9}$$

in which δK, δU and δW are the virtual kinematic, strain energies and virtual work done by the external forces applied on the plate. The variation of strain energy of the nanoplate can be stated as

$$\delta U = \int_A \int_{-\frac{h}{2}}^{\frac{h}{2}} \left[\sigma_{xx}\delta\varepsilon_{xx} + \sigma_{yy}\delta\varepsilon_{yy} + \sigma_{xy}\delta\varepsilon_{xy}\right] dz dA \tag{10}$$

The variation of virtual work done by the external forces

$$\delta W = \int_A F_{Tx}\left(\frac{\partial\delta u}{\partial x} + \frac{\partial w}{\partial x}\frac{\partial\delta w}{\partial x}\right) + F_{Ty}\left(\frac{\partial\delta v}{\partial y} + \frac{\partial w}{\partial y}\frac{\partial\delta w}{\partial y}\right) + 2F_{Txy}\delta\left(\frac{\partial w}{\partial x}\frac{\partial w}{\partial y}\right) + q\delta w + f_x\delta u + f_y\delta v dA \tag{11}$$

where F_{Tx} represents axial compressive force about *x*-axis, and F_{Ty} represents axial compressive force about *y*-axis, F_{Txy} is the external shear force, *q* is the transverse distributed load, f_x, f_y are the distributed axial load along the *x* and *y*, respectively.

The variation of kinetic energy is obtained as

$$\delta K = \int_\Omega \left[\rho\left(\left(\frac{\partial u}{\partial t} - z\frac{\partial^2 w}{\partial x\partial t}\right)\left(\frac{\partial\delta u}{\partial t} - z\frac{\partial^2\delta w}{\partial x\partial t}\right) + \left(\frac{\partial v}{\partial t} - z\frac{\partial^2 w}{\partial y\partial t}\right)\left(\frac{\partial\delta v}{\partial t} - z\frac{\partial^2\delta w}{\partial y\partial t}\right) + \frac{\partial w}{\partial t}\frac{\partial\delta w}{\partial t}\right)\right] dV \tag{12}$$

where ρ is mass density.

By substituting Eqs. (10)-(12) into Eq. (9), then integrating by parts and setting the coefficient δu, δv, δw to zero lead to the following governing equations

$$\frac{\partial N_{yy}}{\partial y} + \frac{\partial N_{xy}}{\partial x} = \rho h\frac{\partial^2 v}{\partial t^2} - f_x \tag{13}$$

$$\frac{\partial N_{xx}}{\partial x} + \frac{\partial N_{xy}}{\partial y} = \rho h\frac{\partial^2 u}{\partial t^2} - f_y \tag{14}$$

$$\begin{aligned}&\frac{\partial^2 M_{xx}}{\partial x^2} + 2\frac{\partial^2 M_{xy}}{\partial x\partial y} + \frac{\partial^2 M_{yy}}{\partial y^2} + F_{Tx}\frac{\partial^2 w}{\partial x^2} + 2F_{Txy}\frac{\partial^2 w}{\partial x\partial y} + F_{Ty}\frac{\partial^2 w}{\partial y^2}\\ &= \rho h\frac{\partial^2 w}{\partial t^2} - \frac{\rho h^3}{12}\left(\frac{\partial^4 w}{\partial x^2\partial t^2} + \frac{\partial^4 w}{\partial y^2\partial t^2}\right)\end{aligned} \tag{15}$$

Substituting Eqs. (7) and (8) into Eq. (5), the correlations between the moment of nonlocal

elasticity and displacement can be expressed by

$$M_{xx} = -D\sum_{k=0}^{\infty}\left(e_0 a\right)^{2k}\nabla^{2k}\left(\frac{\partial^2 w}{\partial x^2}+\mu\frac{\partial^2 w}{\partial y^2}\right) \tag{16a}$$

$$M_{yy} = -D\sum_{k=0}^{\infty}\left(e_0 a\right)^{2k}\nabla^{2k}\left(\frac{\partial^2 w}{\partial y^2}+\mu\frac{\partial^2 w}{\partial x^2}\right) \tag{16b}$$

$$M_{xy} = -D\sum_{k=0}^{\infty}\left(e_0 a\right)^{2k}\nabla^{2k}\left(1-\mu\right)\left(\frac{\partial^2 w}{\partial x\partial y}\right) \tag{16c}$$

where $D = \dfrac{Eh^3}{12\left(1-\mu^2\right)}$ is the bending stiffness of the nanoplate.

Substituting Eq. (16) into Eq. (15), one yields the governing equation of the graphene nanoplate model as

$$\begin{aligned} D\sum_{k=0}^{\infty}\left(e_0 a\right)^{2k}\nabla^{2k}\left(\frac{\partial^4 w}{\partial x^4}+2\frac{\partial^4 w}{\partial x^2\partial y^2}+\frac{\partial^4 w}{\partial y^4}\right) &= \left(F_{Tx}\frac{\partial^2 w}{\partial x^2}+2F_{Txy}\frac{\partial^2 w}{\partial x\partial y}+F_{Ty}\frac{\partial^2 w}{\partial y^2}\right. \\ &\left.+q+\frac{1}{12}\rho h^3\left(\frac{\partial^4 w}{\partial x^2\partial t^2}+\frac{\partial^4 w}{\partial y^2\partial t^2}\right)-\rho h\frac{\partial^2 w}{\partial t^2}\right) \end{aligned} \tag{17}$$

3. Bending, buckling and vibration analyses

In this section, the isotropic graphene nanosheets with simply supported constraints are taken as examples, the analytical solutions of bending, buckling, free and forced vibrations are determined using nonlocal nanoplate model.

Firstly, the boundary conditions of simply supported plates are given by

$$\left(w\right)_{x=0,a} = 0, \left(\frac{\partial^2 w}{\partial x^2}\right)_{x=0,a} = 0 \tag{18a}$$

$$\left(w\right)_{y=0,b} = 0, \left(\frac{\partial^2 w}{\partial x^2}\right)_{y=0,b} = 0 \tag{18b}$$

3.1 bending

For the static bending problem, F_{Tx}, F_{Ty} F_{Txy} f_x f_y and all time derivatives are set to zero. Also, the applied transverse load q is expanded in Fourier series as

$$q_{(x,y)} = \sum_{m=1}^{\infty}\sum_{n=1}^{\infty} Q_{mn} \sin\frac{m\pi x}{a}\sin\frac{n\pi y}{b} \tag{19}$$

$$Q_{mn} = \frac{4}{ab}\int_0^a\int_0^b q_{(x,y)} \sin\frac{m\pi x}{a}\sin\frac{n\pi y}{b}\,dxdy \tag{20}$$

where Q_{mn} are the Fourier coefficients, given as follows

$$q_{(x,y)} = q_0 : Q_{mn} = \frac{16q_0}{mn\pi^2} \quad (m,n=1,3,5...) \tag{21}$$

for uniform load, and

$$q_{(x,y)} = p_0\delta(x-x_p)(y-y_p) : Q_{mn} = \frac{4p_0}{mn}\sin\frac{m\pi x}{a}\sin\frac{n\pi y}{b} \quad (m,n=1,2,3...) \tag{22}$$

for point load, where q_0 is the intensity of the uniformly distributed load, $\delta(\cdot)$ is the Dirac delta function, p_0 is the magnitude of the point load, x_p, y_p are the application position of the point load. When the point load is acted on the midspan of the plate, namely, $q_{(x,y)} = p_0\delta(x-\frac{a}{2})(y-\frac{b}{2})$, the Fourier coefficients have the following form

$$Q_{mn} = \frac{4p_0}{ab}\sin\frac{m\pi}{2}\sin\frac{n\pi}{2} \quad (m, n=1,2,3...) \tag{23}$$

Based on Navier solution procedure, Fourier series function for deflection w is assumed as

$$w = \sum_{m=1}^{\infty}\sum_{n=1}^{\infty} C_{mn} \sin\left(\frac{m\pi}{a}x\right)\sin\left(\frac{n\pi}{b}y\right) \quad (m, n=1,2,3,4\ldots\ldots) \tag{24}$$

where C_{mn} is the Fourier coefficients.

Substituting Eqs. (19)-(21) and (24) into Eq. (17), one obtains

$$C_{mn} = \frac{16q_0}{\sum_{k=0}^{\infty}(-1)^k(e_0a)^{2k}\left[(\frac{m\pi}{a})^2+(\frac{n\pi}{b})^2\right]^k \pi^6 Dmn(\frac{m^2}{a^2}+\frac{n^2}{b^2})^2} \quad (m, n=1,3,5...) \tag{25}$$

Substituting Eq. (25) into Eq. (24), the bending deflection can be rewritten as

$$w = \frac{16q_0}{\pi^6 D}\sum_{m=1,3,5..}^{\infty}\sum_{n=1,3,5..}^{\infty}\sum_{k=0}^{\infty} \frac{1}{(-1)^k(e_0a)^{2k}\left[(\frac{m\pi}{a})^2+(\frac{n\pi}{b})^2\right]^k mn\left[\frac{m^2}{a^2}+\frac{n^2}{b^2}\right]^2}\sin\left(\frac{m\pi}{a}x\right)\sin\left(\frac{n\pi}{b}y\right) \tag{26}$$

The maximal transverse deflection occurs at $x=\frac{a}{2}$, $y=\frac{b}{2}$, and by setting $e_0a=0$, the classical deflection solution can be recovered as

$$w_{\max}^{L}=\frac{16q_0}{\pi^6 D}\sum_{m=1,3,5..}^{\infty}\sum_{n=1,3,5..}^{\infty}\frac{1}{mn(\frac{m^2}{a^2}+\frac{n^2}{b^2})^2} \tag{27}$$

The ratio of the nonlocal deflection to classical one is

$$\frac{w_{\max}}{w_{\max}^{L}}=\frac{\sum_{m=1,3,5..}^{\infty}\sum_{n=1,3,5..}^{\infty}\sum_{k=0}^{\infty}\frac{1}{(-1)^k(e_0a)^{2k}\left[(\frac{m\pi}{a})^2+(\frac{n\pi}{b})^2\right]^k mn(\frac{m^2}{a^2}+\frac{n^2}{b^2})^2}}{\sum_{m=1,3,5..}^{\infty}\sum_{n=1,3,5..}^{\infty}\frac{1}{mn(\frac{m^2}{a^2}+\frac{n^2}{b^2})^2}}\quad (m,n=1,3,5\cdots) \tag{28}$$

3.2 Free and forced vibrations

For free vibration we set F_{Tx}, F_{Ty}, F_{Txy}, f_x, f_y, q to zero, but the bending deflection is the function of time. The deflection for free vibration of nanoplate can be written as

$$w_0=\sum_{m=1}^{\infty}\sum_{n=1}^{\infty}T_{mn}(t)W_{mn}(x,y) \tag{29}$$

Substituting Eq. (29) into Eq. (17) and using the conditions of free vibration of nanoplate yields

$$DT_{mn}\nabla^4 W_{mn}=\frac{1}{\sum_{k=0}^{\infty}(e_0a)^{2k}\nabla^{2k}\frac{1}{\left[\frac{\rho h^3}{12}(\frac{\partial^2 W_{mn}}{\partial x^2}\frac{\partial^2 T_{mn}}{\partial t^2}+\frac{\partial^2 W_{mn}}{\partial y^2}\frac{\partial^2 T_{mn}}{\partial t^2})-\rho h\frac{\partial^2 T_{mn}}{\partial t^2}W_{mn}\right]}} \tag{30}$$

For simply supported nanoplate T_{mn} can be expressed as

$$T_{mn}=A_{mn}\sin\omega_{mn}t+B_{mn}\cos\omega_{mn}t \tag{31}$$

here ω_{mn} is the circular frequency of free vibration of graphene nanosheets.

Substituting Eq. (31) into Eq. (30) leads to the following equation

$$D\nabla^4 W_{mn}=\frac{1}{\sum_{k=0}^{\infty}(e_0a)^{2k}\nabla^{2k}\frac{1}{\left[\rho hW_{mn}-\frac{\rho h^3}{12}(\frac{\partial^2 W_{mn}}{\partial x^2}+\frac{\partial^2 W_{mn}}{\partial y^2})\right]\omega_{mn}^2}} \tag{32}$$

Shape function of free vibration can be written as

$$W_{mn}=\sin\frac{m\pi x}{a}\sin\frac{n\pi y}{b} \tag{33}$$

By substituting Eq. (33) into Eq. (32) and considering a non-trivial solution of the system, the circular frequencies of the graphene nanosheet can be expressed as

$$\omega_{mn}^2 = \frac{\sum_{k=0}^{\infty}(-1)^k(e_0a)^{2k}\left[(\frac{m\pi}{a})^2+(\frac{n\pi}{b})^2\right]^k D\left[(\frac{m\pi}{a})^2+(\frac{n\pi}{b})^2\right]^2}{\left(\frac{\rho h^3}{12}\left[(\frac{m\pi}{a})^2+(\frac{n\pi}{b})^2\right]+\rho h\right)} \tag{34}$$

When the nonlocal parameter e_0a vanishes, Eq. (34) reduces to the classical results $\left(\omega_{mn}^L\right)^2$

Considering the graphene nanosheets subjected to dynamic loads, namely the forced vibration, the differential equations of motion are similar to the free vibration, but q is not equal to zero, and it can be assumed as

$$q=q_t(x,y)\cos\omega t \tag{35}$$

Using Eqs. (19)-(21), $q_t(x,y)$ can be expanded in Fourier series as

$$q_t(x,y)=\sum_{m=1,3,5,\ldots}^{\infty}\sum_{n=1,3,5,\ldots}^{\infty}\frac{16q_0}{\pi^2mn}\sin\frac{m\pi x}{a}\sin\frac{n\pi x}{b} \tag{36}$$

The transverse deflection is assumed as

$$w_1=\sum_{m=1}^{\infty}\sum_{n=1}^{\infty}T_{1mn}(t)W_{mn}(x,y) \tag{37}$$

Substituting Eq. (37) into Eq. (17) with the conditions of forced vibration yields

$$T_{1mn}(D\nabla^4W_{mn})-\frac{1}{\sum_{k=0}^{\infty}(e_0a)^{2k}\nabla^{2k}\frac{1}{\left[\frac{\rho h^3}{12}(\frac{\partial^2W_{mn}}{\partial x^2}\frac{\partial^2T_{1mn}}{\partial t^2}+\frac{\partial^2W_{mn}}{\partial y^2}\frac{\partial^2T_{1mn}}{\partial t^2})-\rho h\frac{\partial^2T_{1mn}}{\partial t^2}W_{mn}\right]}}=q \tag{38}$$

The dynamic load can be expanded in the series form with respect to the shape function as

$$q(x,y,t)=\sum_{m=1}^{\infty}\sum_{n=1}^{\infty}F_{mn}(t)W_{mn}(x,y) \tag{39}$$

From the Eqs. (36) and (39), we can obtain

$$F_{mn}=\frac{16q_0}{\pi^2mn}\cos\omega t \quad (m,n=1,3,5\ldots) \tag{40}$$

On the other hand, T_{1mn} can be assumed as

$$T_{1mn}=A_{mn}\sin\omega_{mn}t+B_{mn}\cos\omega_{mn}t+\tau_{mn} \tag{41}$$

Substituting Eqs. (32), (33), (39), (40) and (41) into Eq. (38) we can obtain one particular solution for τ_{mn} is

$$\tau_{mn}=\frac{\sum_{k=0}^{\infty}(-1)^k(e_0a)^{2k}\left[(\frac{m\pi}{a})^2+(\frac{n\pi}{b})^2\right]^k\frac{16q_0}{mn\pi^2}\cos\omega t}{\left(\rho h+\frac{\rho h^3}{12}[(\frac{m\pi}{a})^2+(\frac{n\pi}{b})^2]\right)\left(\omega_{mn}^2-\omega^2\right)} \tag{42}$$

Substituting Eqs. (33), (41), and (42) into Eq. (37) yields

$$\begin{aligned}w_1=&\sum_{m=1,3,5\ldots}^{\infty}\sum_{n=1,3,5\ldots}^{\infty}[A_{mn}\sin\omega_{mn}t+B_{mn}\cos\omega_{mn}t+\\&\frac{\sum_{k=0}^{\infty}(-1)^k(e_0a)^{2k}\left[(\frac{m\pi}{a})^2+(\frac{n\pi}{b})^2\right]^k\frac{16q_0}{mn\pi^2}\cos\omega t}{\left(\rho h+\frac{\rho h^3}{12}[(\frac{m\pi}{a})^2+(\frac{n\pi}{b})^2]\right)\left(\omega_{mn}^2-\omega^2\right)}]\sin\frac{m\pi x}{a}\sin\frac{n\pi y}{b}\end{aligned} \tag{43}$$

The initial conditions can be expressed as

$$\left(w_1\right)_{t=0}=0,\left(\frac{\partial w_1}{\partial t}\right)_{t=0}=0 \tag{44}$$

where the graphene nanosheets are initially in equilibrium position. Substituting Eq. (44) into (43) yields

$$w_1=\sum_{m=1,3,5\ldots}^{\infty}\sum_{n=1,3,5\ldots}^{\infty}\sum_{k=0}^{\infty}\left[\frac{(-1)^k(e_0a)^{2k}\left[(\frac{m\pi}{a})^2+(\frac{n\pi}{b})^2\right]^k\frac{16q_0}{mn\pi^2}(\cos\omega t-\cos\omega_{mn}t)}{\left(\rho h+\frac{\rho h^3}{12}[(\frac{m\pi}{a})^2+(\frac{n\pi}{b})^2]\right)\left(\omega_{mn}^2-\omega^2\right)}\right]\sin\frac{m\pi x}{a}\sin\frac{n\pi y}{b} \tag{45}$$

3.3 Buckling

For the buckling analyses, the initial force can be expressed as follows

$$F_{Tx}=-F_x,\ \ F_{Ty}=0,\ \ F_{Txy}=0,\ \ f_x=0,\ \ f_y=0,\ \ q=0,\frac{\partial^2 w}{\partial t^2}=0 \tag{46}$$

Using Eqs.(17), (24) and (46), one can arrive at

$$\sum_{m=1}^{\infty}\sum_{n=1}^{\infty}C_{mn}\left(D\left[\left(\frac{m\pi}{a}\right)^2+\left(\frac{n\pi}{b}\right)^2\right]^2-\frac{F_x\left(\frac{m\pi}{a}\right)^2}{\sum_{k=0}^{\infty}(-1)^k(e_0a)^{2k}\left[(\frac{m\pi}{a})^2+(\frac{n\pi}{b})^2\right]^k}\right)\sin\frac{m\pi x}{a}\sin\frac{n\pi x}{b}=0 \tag{47}$$

The solution of Eq. (47) can be determined as

$$F_x = \frac{D\sum_{k=0}^{\infty}(-1)^k(e_0a)^{2k}\left[(\frac{m\pi}{a})^2+(\frac{n\pi}{b})^2\right]^k\left[\left(\frac{m\pi}{a}\right)^2+\left(\frac{n\pi}{b}\right)^2\right]^2}{\left(\frac{m\pi}{a}\right)^2} \tag{48}$$

It is noticed that Eq. (48) reduces to the corresponding classical results without the nonlocal parameter e_0a.

In order to reveal the effects of nonlocal parameter, half wave number and three-dimensional sizes on the static and dynamic responses of the graphene nanosheets in detail, the parameters including Yong's modulus E=1.06TPa, Poisson's ratio μ=0.25 and mass density ρ=2250 kg/m^3 are adopted. Meanwhile, the natural frequencies can be directly obtained from Eq. (49) as

$$f_{mn} = \frac{\omega_{mn}}{2\pi} = \frac{1}{2\pi}\sqrt{\frac{K_{mn}}{M_{mn}}} \tag{49}$$

In which K_{mn}, M_{mn} are equivalent rigidity and mass respectively, as

$$K_{mn} = D\sum_{k=0}^{\infty}(-1)^k(e_0a)^{2k}\left[(\frac{m\pi}{a})^2+(\frac{n\pi}{b})^2\right]^k D\left[(\frac{m\pi}{a})^2+(\frac{n\pi}{b})^2\right]^2$$

$$M_{mn} = \left(\frac{\rho h^3}{12}\left[(\frac{m\pi}{a})^2+(\frac{n\pi}{b})^2\right]+\rho h\right)$$

Firstly, to demonstrate the efficiency and accuracy of the present analytical solutions, some illustrative examples are solved and compared using the data available in literatures. For this purpose, frequency ratio f_L/f is defined as the ratio of the fundamental frequency of the classical plate to that of the nonlocal plate. Table 1 shows the calculations of frequency ratio, where the properties of the graphene nanosheets are the same as those in Refs (Reddy 2007, Eltaher *et al*. 2013). It is clear from Table 1 that the present results are in good agreement with the literatures (Reddy 2007, Eltaher *et al*. 2013).

Table 1 Comparison of the ratio of the classical fundamental frequency to nonlocal counterpart between the present work and Refs (Reddy 2007, Eltaher *et al*. 2013) (h=0.34 nm, a=b=10 nm)

$(e_0a)^2$ (nm^2)	f_L/f (present)	f_L/f (Reddy 2007)	f_L/f (Eltaher *et al*. 2013)
0	1	1	1
1	1.0942	1.0924	1.0942
2	1.1811	1.1811	1.1809
3	1.2618	1.2618	1.2617

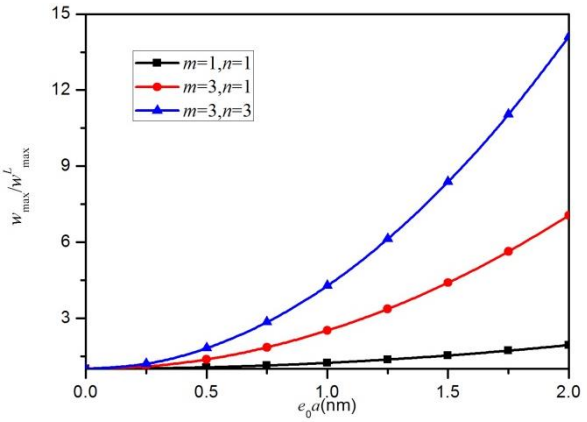

Fig. 1 The ratio of nonlocal to classical maximum deflections versus nonlocal parameter and half wave number (a=b=10 nm)

Fig. 1 shows the ratio of maximum deflection versus m and n on the effect of nonlocal parameter. It is seen m and n have the site symmetry from Eq. (28). So m=1, n=3 are the same as n=1, m=3. It is observed that increasing m or n causes $w_{\max}/w^L_{\max}$ to increase, this is because $w_{\max}$ increase faster than $w^L_{\max}$ with the increase of half wave number.

Fig. 2 shows the ratio of maximum deflection versus a and b on the effect of nonlocal parameter. It is seen that a and b also have site symmetry from Fig. 2, and a=10 nm, b=20 nm are the same as a=20 nm, b=10 nm. It is different from Fig. 1 that $w_{\max}/w^L_{\max}$ decreases with the increase of a and b. In addition h has no effect on $w_{\max}/w^L_{\max}$. Both of Figs. 1 and 2 prove that $w_{\max}/w^L_{\max}$ increases with increasing e_0a.

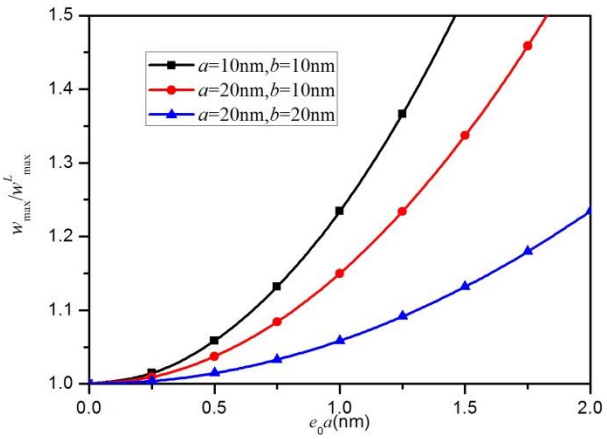

Fig. 2 The ratio of nonlocal to classical maximum deflections versus length, width and nonlocal parameter (m=n=1)

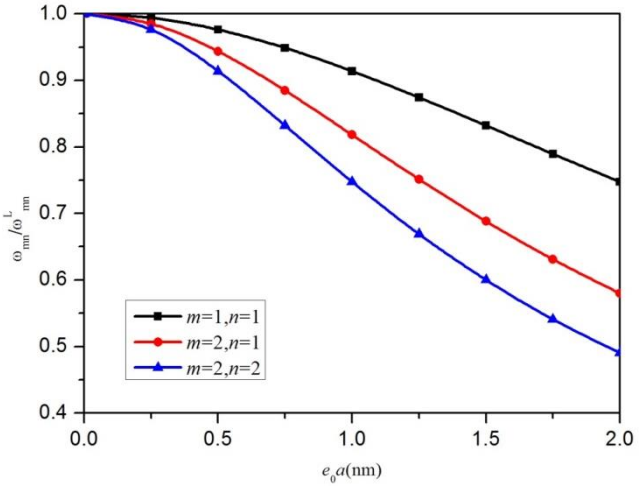

Fig. 3 Change of ratio of the nonlocal to classical circular frequencies with half wave number for different nonlocal parameters (a=b=10 nm)

As a significant result, Figs. 3 and 4 show that the change of ratio of the circular frequencies of the nonlocal nanosheets to those of classical plates. It is observed that $\omega_{mn}/\omega_{mn}^{L}$ decreases with the increase of half wave number *m* and *n*, but it increases with the increase of length and width *a* and *b*. From Figs. 3 and 4, it is concluded that the $\omega_{mn}/\omega_{mn}^{L}$ decreases by increasing the e_0a. In addition, it is seen that $\omega_{mn}/\omega_{mn}^{L}$ drops rapidly when e_0a is very small.

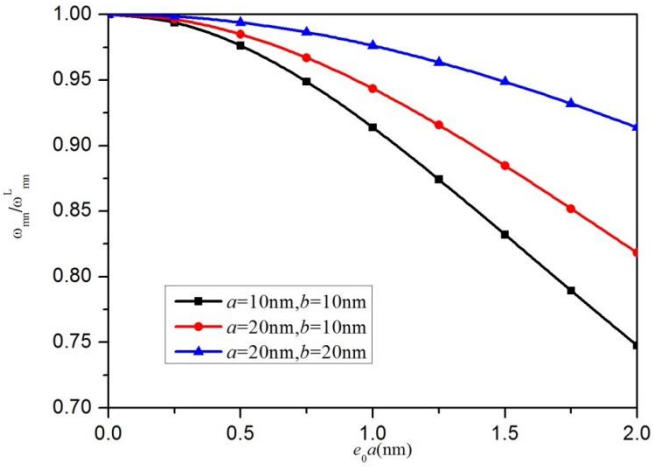

Fig. 4 Change of ratio of the nonlocal to classical circular frequencies with length and width for different nonlocal parameters (m=n=1)

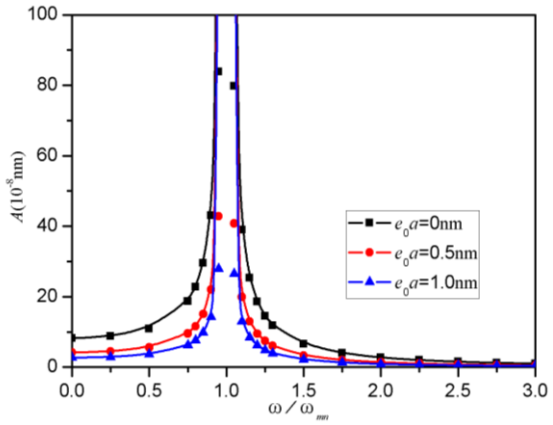

Fig. 5 The variation of relative amplitude against the nonlocal parameter with different circular frequencies ratios (a=b=10nm, h=0.34nm, m=n=1)

In order to present numerical result in a comparable form, the following relative amplitude is defined as

$$A=\left|\sum_{m=1,3,5\ldots}^{\infty}\sum_{1=1,3,5\ldots}^{\infty}\sum_{k=0}^{\infty}\frac{(-1)^k(e_0a)^{2k}\left[(\frac{m\pi}{a})^2+(\frac{n\pi}{b})^2\right]^k}{mn\left(\rho h+\frac{\rho h^3}{12}\left[\left(\frac{m\pi}{a}\right)^2+\left(\frac{n\pi}{b}\right)^2\right]\right)\left(\omega^2-\omega_{mn}^2\right)}\right|$$

Figs. 5-8 highlight the effects of main parameters including nonlocal parameters, half wave number, three-dimensional sizes on relative amplitude. It can be seen from Figs. 6 and 8 that as the *m*, *n*, *a*, *b* increase, the relative amplitude *A* increases. It is observed from Figs. 5 and 7 that relative amplitude *A* decreases with the increase of e_0a and *h*. From all of these figures we can also find that no matter what e_0a, *m*, *n*, *a*, *b* values, when ω/ω_{mn} tends to 1, *A* tends to infinity that is well-know resonance phenomenon. On the other hand, when ω/ω_{mn} tends to infinity, relative amplitude converges to zero.

From Eq. (48) we find that *m*, *n* and *a*, *b* donot have site symmetry in the expression of F_x. The transverse load with half wave number for different nonlocal parameters is depicted in Fig. 9, where the minimum transverse load is obtained when the values of *m* and *n* are equal to one. That is, setting all the half wave number to one the critical buckling load F_{xcr} can be obtained. Figs. 10 and 11 show the variation of critical bucking load with three-dimensional sizes for different nonlocal parameters. It is concluded F_{xcr} increases with the increase of *h* from Fig. 10, that is mainly attributed to increasing *h* causes the bending stiffness to increase. It is clear that from Fig. 11 F_{xcr} increases with the increase of *b*, but decreases with the increase of *a*. From Figs. 10 and 11 it is indicated that F_{xcr} drops rapidly with the increase of e_0a.

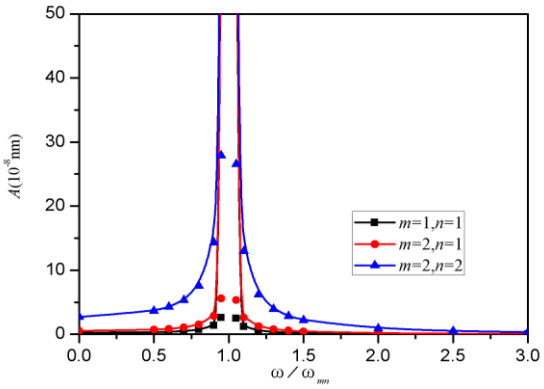

Fig. 6 The variation of relative amplitude against the half wave number with different circular frequencies ratios (a=b=10 nm,h=0.34 nm, e_0a=1 nm)

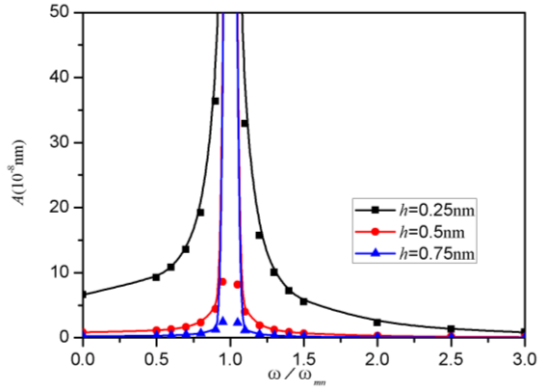

Fig. 7 The variation of relative amplitude against the thickness with different circular frequencies ratios (a=b=10nm, m=n=1, e_0a=1 nm)

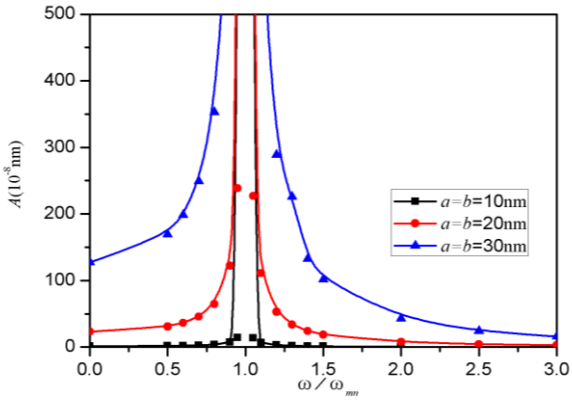

Fig. 8 The variation of relative amplitude against the length and width with different circular frequencies ratios (h=0.34nm, m=n=1, e_0a=1 nm)

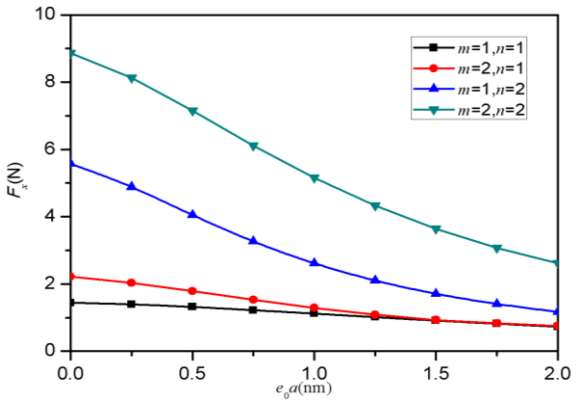

Fig. 9 Variation transverse load with half wave number for different nonlocal parameters (h=0.34 nm, a=b=10 nm)

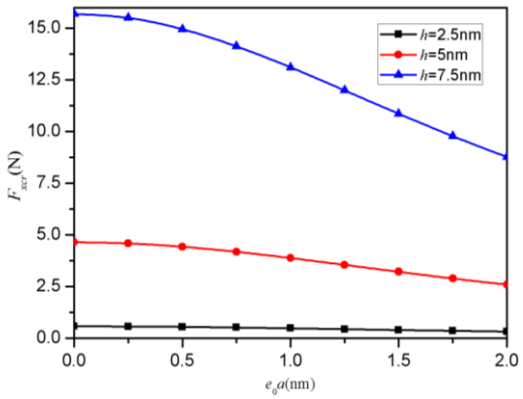

Fig. 10 Variation of critical bucking load with thickness for different nonlocal parameters (m=n=1, a=b=10 nm)

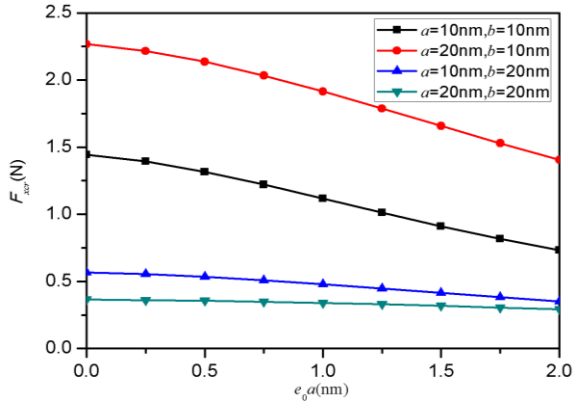

Fig. 11 Variation of critical bucking load with length and width for different nonlocal parameters (h=0.34 nm, m=n=1)

4. Conclusions

Governing equations of bending, buckling, free and forced vibrations of graphene nanosheets are derived based nonlocal elastic plate constitutive. The numerical results for simply supported nanoplate model are addressed in detail. It is shown that the deflection increases, but the natural frequency, amplitude of forced vibration and the critical bucking load decrease with an increase in nonlocal parameter. Increasing the half wave number causes the deflection and amplitude to increase. The thickness of the nanoplate has no effect on deflection while the amplitude of forced vibration and critical bucking load decrease with the increase of thickness. The deflection decreases but the amplitude increases with the increase of length and width. For the critical bucking load, it is found to increase with the increase of length, but decrease with the increase of width. The present results are expected to be useful for understanding the static and dynamic behaviors accounting for nonlocal small scale effect of two-dimensional nanostructures.

Acknowledgements

The authors are grateful for funding supports from the Soochow Scholar Programme of Soochow University, the National Natural Science Foundation of China (No. 51406128), the Natural Science Foundation of Jiangsu Province (Nos. BK20140342, BK20130303) and the project from Suzhou Bureau of Science and Technology (No. SYG201537).

References

Aydogdu, M. (2009), "A general nonlocal beam theory: its application to nanobeam bending, buckling and vibration", *Phys. E*., **41**(9), 1651-1655.

Bedroud, M., Nazemnezhad, R. and Hosseini-Hashemi, S. (2015), "Axisymmetric/ asymmetric buckling of functionally graded circular/annular Mindlin nanoplates via nonlocal elasticity", *Meccanica*, **50**, 1791-1806.

Eberhardt, O. and Wallmersperger, T. (2014), "Mechanical properties and deformation behavior of carbon nanotubes calculated by a molecular mechanics approach", *Smart Struct. Syst*., **13**(4), 685-709.

Eltaher, M.A., Emam, S.A. and Mahmoud, F.F. (2013), "Static and stability analysis of nonlocal functionally graded nanobeams", *Compos Struct*., **96**, 82-88.

Eringen, A.C. and Edelen, D. (1972), "On nonlocal elasticity", *Int. J. Eng. Sci*., **10**(3), 233-248.

Eringen, A.C. (1983), "On differential equations of nonlocal elasticity and solutions of screw dislocation and surface waves", *J. Appl. Phys*., **54**(9), 4703-4710.

Hosseini-Hashemi, S., Kermajani, M. and Nazemnezhad, R. (2015), "An analytical study on the buckling and free vibration of rectangular nanoplates using nonlocal third-order shear deformation plate theory", *Eur. J. Mech. A - Solids*., **51**, 29-43.

Hosseini, M., Sadeghi-Goughari, M., Atashipour, S.A. and Eftekhari, M. (2014), "Vibration analysis of single-walled carbon nanotubes conveying nanoflow embedded in a viscoelastic medium using modified nonlocal beam model", *Arch. Mech*., **66**(4), 217-244.

Liew, K.M., He, X.Q. and Kitipornchai, S. (2006), "Predicting nanovibration of multi-layered graphene sheets embedded in an elastic matrix", *Acta. Mater*., **54**(16), 4229-4236.

Li, C., Lim, C.W. and Yu, J.L. (2011), "Dynamics and stability of transverse vibrations of nonlocal nanobeams with a variable axial load", *Smart Mater. Struct*., **20**(1), 015023.

Murmu, T. and Pradhan, S.C. (2009), "Small-scale effect on the vibration of nonuniform nanocantilever

based on nonlocal elasticity theory", *Physica. E*., **41**(8), 1451-1456.
Pradhan, S.C. and Phadikar, J.K. (2009), "Nonlocal elasticity theory for vibration of nanoplates", *J. Sound Vib*., **325**(1), 206-223.
Pradhan, S.C. and Kumar, A. (2011), "Vibration analysis of orthotropic graphene sheets using nonlocal elasticity theory and differential quadrature method", *Compos. Struct*., **93**(2), 774-779.
Reddy, J.N. (2007), "Nonlocal theories for bending, buckling and vibration of beams", *Int. J. Eng. Sci*., **45**(2), 288-307.
Sahmani, S. and Bahrami, M. (2015), "Nonlocal plate model for dynamic pull-in instability analysis of circular higher-order shear deformable nanoplates including surface stress effect", *J. Mech. Sci. Tech*., **29**(3), 1151-1161.
Shen, Z.B., Tang, H.L., Li, D.K. and Tang, G.J. (2012), "Vibration of single-layered graphene sheet-based nanomechanical sensor via nonlocal Kirchhoff plate theory", *Comput. Mater. Sci*., **61**, 200-205.
Şimşek, M. and Yurtcu, H.H. (2013), "Analytical solutions for bending and buckling of functionally graded nanobeams based on the nonlocal Timoshenko beam theory", *Compos. Struct*., **97**, 378-386.
Yan, J.W., Tong, L.H., Li, C., Zhu, Y. and Wang, Z.W. (2015), "Exact solutions of bending deflections for nano-beams and nano-plates based on nonlocal elasticity theory", *Compos. Struct*., **125**, 304-313.
Yin, F., Chen, C.P. and Chen, D.L. (2015), "Vibration analysis of nano-beam with consideration of surface effects and damage effects", *Nonlinear Eng*., **4**(1), 61-66.
Zhang, Y., Zhang, L.W., Liew, K.M. and Yu, J.L. (2015), "Transient analysis of single-layered graphene sheet using the kp-Ritz method and nonlocal elasticity theory", *Appl. Math. Comput*., **258**, 489-501.
Zhang, Y., Lei, Z.X., Zhang, L.W., Liew, K.M. and Yu, J.L. (2015), "Nonlocal continuum model for vibration of single-layered graphene sheets based on the element-free kp-Ritz method", *Eng. Anal. Bound. Elem*., **56**, 90-97.

CY